

# Possible charge ordered states in BN (BCN) nanotubes and nanoribbons

Kikuo Harigaya\*

*Nanotechnology Research Institute, AIST, Tsukuba 305-8568, Japan*<sup>†</sup>

*Synthetic Nano-Function Materials Project, AIST, Tsukuba 305-8568, Japan*

(Received )

## Abstract

Electronic states in boron-nitride and boron-carbon-nitride nanoribbons with zigzag edges are studied using the extended Hubbard model with nearest neighbor Coulomb interactions. The charge and spin polarized states are considered, and the phase diagram between two states is obtained. Next, the electric capacitance is calculated in order to examine the nano-functionalities of the system. Due to the presence of the strong site energies, the charge polarized state overcomes the spin polarized states, giving the large difference of the phase diagram in comparison with that of graphite system. The electronic structures are always like of semiconductors. The capacitance calculated for the charge polarized state with the realistic values of the Coulomb interactions is inversely proportional to the ribbon width, owing to the presence of the charge excitation energy gap.

PACS numbers: 71.10.Hf, 73.22.-f, 73.20.At, 77.22.Ej

---

\*E-mail address: [k.harigaya@aist.go.jp](mailto:k.harigaya@aist.go.jp); URL: <http://staff.aist.go.jp/k.harigaya/>

<sup>†</sup>Corresponding address

# I. Introduction

Nano-carbon (C) materials and hetero-materials including borons (B) and nitrogens (N) have been attracting much attention both in the fundamental science and in the interests of application to nanotechnology devices [1,2]. Their physical and chemical natures change variously depending on geometries [1-3]. In carbon nanotubes, diameters and chiral arrangements of hexagonal pattern on tubules decide whether they are metallic or not [1,2].

In nanographites, the edge atoms strongly affect the electronic states [3], and there are nonbonding molecular orbitals localized mainly along the zigzag edges. Recently, we have studied the competition between the spin and charge orderings due to the on-site and nearest neighbor Coulomb interactions [4]. The nearest neighbor Coulomb interaction stabilizes the charge polarized (CP) state with a finite electric dipole moment in zigzag ribbons, and it competes with the spin polarized (SP) state. It has been discussed that the transverse electric field might induce the first order phase transition from the SP state to the CP state.

In view of these findings, it is interesting to perform further theoretical investigations for BN (BCN) nanotubes and nanoribbons. The BN systems are hetero-atom materials, where B and N are located alternatively on the honeycomb lattice. The BN plane and nanotubes are intrinsic insulators with the energy gap about 4 eV [5,6]. Low energy excitation properties have not been investigated so much. We will discuss interplay between CP and SP states, even though there remain limitations of theories of a single orbital only. We note that photogalvanic effects have been discussed using the single orbital theory [7]. Our idea is similar to this study, and we will introduce site energies at the B and N sites. The other system, BCN nanotubes and nanoribbons, is a model material, where B atoms are arrayed along one edge and N atoms along the other edge. The experiments of the low concentration limit of B and/or N doping into carbon nanotubes have sometimes suggested accumulation of impurity atoms at edge sites [8,9]. The formation of zigzag nanotubes is favored. We will consider electronic properties of zigzag BCN nanoribbons, too.

We will discuss that spin excitations tend to be suppressed due to the presence of the large energy gap. This gives rise to the enlarged region of the CP state in the phase diagrams of the BN and BCN systems. This property is largely in contrast to the dominant SP state of the zigzag graphite ribbons [4].

The next interest of this paper is how such the electronic properties appear in measurable quantities. We will consider electric capacitance because the CP state is accompanied with dielectric moment with respect to the charge orders. We model the periodic zigzag ribbon as a “nano-size condenser”, where a set of the B edge atoms are regarded as a positive electrode, a set of the N edge atoms as a negative electrode, and a material as a spacer is present between the positive and negative electrodes. The “differential capacitance” will be calculated as a response of charge with respect to the weak static field applied to the system in the transverse direction. The similar idea of the calculations has been used in the study using the first principle methods [10]. We find that the calculated capacitance is inversely proportional to the distance between the positive and negative electrode. This behavior could be understood by the presence of an energy gap for charge excitations.

This paper is organized as follows. In Sec. II, we explain the extended Hubbard model, and give the calculation method. In Sec. III, we give results for the BN systems. In Sec. IV, calculations of the BCN systems are reported. The paper is closed with a short summary in Sec. V.

## II. Model and method

Figure 1 illustrates the geometry of zigzag nanoribbons with an inversion symmetry. Here,  $N$  and  $L$  are the width and length of the ribbon, respectively. Figure 1 (a) shows the zigzag BN ribbons, and Fig. 1 (b) shows the zigzag BCN ribbons. The periodic boundary condition is set along the  $y$ -axis parallel to the zigzag-lines. Since the zigzag ribbon is a bipartite,  $A$  (boron) and  $B$  (nitrogen) sites are assigned by the filled and open circles in Fig. 1 (a), respectively.

All the twofold coordinated sites in the lower and upper zigzag edges belong to the *A* and *B* sublattices, respectively, at which edge states are mainly localized. In Fig. 1 (b), the B atoms are present along the upper zigzag edge sites, while there are the N atoms along the lower edges. The inner part is composed of C atoms. The closed, shaded, and open circles are for B, C, and N atoms, respectively. The experiments of the low concentration limit of B and/or N doping into carbon nanotubes have sometimes suggested accumulation of impurity atoms at edge sites [8]. The formation of zigzag nanotubes is favored. Therefore, we choose this structure as a model system.

We treat a half-filled  $\pi$ -electron system on the zigzag ribbon using the extended Hubbard Hamiltonian with the on-site  $U$  and nearest-neighbor  $V$  Coulomb interactions. The model is as follows:

$$\begin{aligned}
H = & E_B \sum_{i \in B, \sigma} c_{i,\sigma}^\dagger c_{i,\sigma} + E_N \sum_{i \in N, \sigma} c_{i,\sigma}^\dagger c_{i,\sigma} \\
& - t \sum_{\langle i,j \rangle, \sigma} (c_{i,\sigma}^\dagger c_{j,\sigma} + \text{h.c.}) + U \sum_i (c_{i,\uparrow}^\dagger c_{i,\uparrow} - \frac{n_{\text{el}}}{2})(c_{i,\downarrow}^\dagger c_{i,\downarrow} - \frac{n_{\text{el}}}{2}) \\
& + V \sum_{\langle i,j \rangle} (\sum_{\sigma} c_{i,\sigma}^\dagger c_{i,\sigma} - n_{\text{el}})(\sum_{\tau} c_{j,\tau}^\dagger c_{j,\tau} - n_{\text{el}}),
\end{aligned} \tag{1}$$

where  $E_B$  and  $E_N$  are the site energies at the B and N sites, respectively; the sum with  $i \in B$  and  $i \in N$  are taken over the B and N atoms, respectively;  $c_{i,\sigma}$  annihilates a  $\pi$ -electron of spin  $\sigma$  at the  $i$ th site;  $t$  ( $> 0$ ) is the hopping integral between the nearest neighbor  $i$ th and  $j$ th sites; the sum with  $\langle i,j \rangle$  is taken for all the pairs of the nearest neighbor sites;  $n_{\text{el}}$  is the average electron density of the system. We adopt the standard Unrestricted Hartree-Fock approximation to this model [4,11]:

$$c_{i,\uparrow}^\dagger c_{i,\uparrow} c_{i,\downarrow}^\dagger c_{i,\downarrow} \Rightarrow \langle c_{i,\uparrow}^\dagger c_{i,\uparrow} \rangle c_{i,\downarrow}^\dagger c_{i,\downarrow} + c_{i,\uparrow}^\dagger c_{i,\uparrow} \langle c_{i,\downarrow}^\dagger c_{i,\downarrow} \rangle - \langle c_{i,\uparrow}^\dagger c_{i,\uparrow} \rangle \langle c_{i,\downarrow}^\dagger c_{i,\downarrow} \rangle. \tag{2}$$

In order to examine nano-functionalities as “nano-size condensers”, electric capacitance of the zigzag ribbons is calculated. We assume that one set of B atoms along the upper zigzag edge is regarded as a positive electrodes. The other set of N atoms along the lower zigzag edge is regarded as a negative electrodes. The absolute value of the net variation of the accumulated

charge is divided by the strength of the small applied voltage, and the capacitance is obtained. The quantity  $Q_0$  is the net charge over the  $L/2$  B or N atoms at the zigzag edge sites, when the static electric field is absent. The part  $dQ$  is the change of the net charge with respect to the small field which is parallel to the  $x$ -axis of Fig. 1 (a). The capacitance  $C$  is calculated using the relation of polarizability  $dQ = CdV$ , where  $dV$  is the change of voltage due to the static electric field. The similar method has been used for the calculation of the capacitance using the first principle techniques recently [10]. Here, we assume that the bond length between carbons is 1.45 Å.

### III. Zigzag BN nanotubes and nanoribbons

We will discuss electronic properties of the zigzag BN nanotubes and nanoribbons. The lattice structure is shown in Fig. 1 (a). The site energies at the B and N are taken to be  $E_B = +t$  and  $E_N = -t$ . The realistic magnitude  $t \sim 2$  eV gives the energy gap  $2t \sim 4$  eV, which has been reported in the band calculations [8,9]. The similar choice of site energies in the single-orbital tight binding model has been done for the random doping of BCN alloys in the literature [12]. The total electron number is same with that of the site number. This ensures the charge neutrality of the system.

Figure 2 (a) shows the typical example of charge density distribution of the CP state for  $U = 1t$  and  $V = 0$ , and Fig. 2 (b) displays the  $z$ -component of spin density distribution of the SP state for  $U = 4t$  and  $V = 0$ . The size of the zigzag ribbon is with  $4 \times 20$  sites. The filled and open circles show positive and negative densities. Their radii are proportional to the magnitudes of the charge or spin densities: the maximum is 0.60 in Fig. 2 (a) and 0.35 in Fig. 2 (b). Due to the strong site energies, there are alternations of electron number density which are extend over the system in Fig. 2 (a). Furthermore, at the B sites along the upper edge, the positive charge density is enhanced than that of the inner part of the ribbon. At the N sites along the lower edges, the negative density becomes enhanced similarly. As the interaction

$U$  becomes stronger, the system changes into the SP state via phase transition. Fig. 2 (b) shows the spin density distributions. The alternations of spins are quite strong owing to the very large interaction parameter. The absolute values of the spin density are enhanced along the two edges. Such the modulations of the CP and SP near the edges are the result of the wavefunctions localized along the edge sites, as we have discussed for graphite ribbons [4].

The total energies of the CP and SP solutions are compared, and the phase diagram of the stable state is given in Fig. 3. The calculation has been done for  $N = 4$  and  $L = 40$ . The phase boundary, denoted by the bold line, indicates the first order phase transition. The dashed line is the strong correlation limit,  $V = N(U + 2E_N)/(3N - 1) = 4(U - 2t)/11$ , which can be obtained by taking the energies of the two states as equal. The bold line approaches to the dashed line, when  $U$  and  $V$  become larger. The strong site energy difference gives rise to huge charge polarizations, as shown in Fig. 2 (a). The region of the CP state extends in the phase diagram, and the SP state is highly suppressed. The realistic values of the interactions might be near to the regions,  $0 < U < 3t$  and  $V \sim 0$ , which correspond to CP states in the phase diagram. For the nanographite ribbon [4], the phase boundary crosses the origin  $(U, V) = (0, 0)$ . So, the SP state has been found in these regions. The strong site energies of the BN system have resulted in the quite remarkable change of ordered states between the graphite and BN systems.

Figure 4 shows the electric capacitance of the zigzag BN ribbons of  $L = 20$  by changing the ribbon width. As the ribbon becomes wider, the system develops into the zigzag (10,0) nanotube. The raw value of the capacitance (a) and the inverse (b) are plotted. We take three parameter sets of Coulomb interactions. The system is in the CP state for these parameters. All the curves exhibit the almost inversely proportional behaviors of the capacitance as functions of the ribbon width. There is a huge electronic gap due to the strong site energy difference. The system is a semiconductor intrinsically. The strong charge excitation energy gap results in the inversely proportional behaviors. Even though the present capacitance is the “differential capacitance”, the dependence on the spacer width is similar to that of the classical parallel electrode condenser. Such the analogy seems interesting in view of the fact that the spacer of

the “nano-condenser” is made of the intrinsic insulator of the BN system.

## IV. Zigzag BCN nanotubes and nanoribbons

In this section, we report electronic properties of the zigzag BCN nanotubes and nanoribbons, comparing with those of the BN systems. The lattice structure of the BCN systems is shown in Fig. 1 (b). In the present calculations, the site energies at the B and N are taken to be  $E_B = +0.8t$  and  $E_N = -0.8t$ . Because the most part of the system is composed of carbons, we take  $t \sim 2.5$  eV. So, the site energies at B and N take the same value as used in the previous section. The total electron number is same with that of the site number again. Note that we have checked that the calculated results change very weakly even when we take the site energies  $E_B = +t$  and  $E_N = -t$ , indicating that the slight change of the site energies is not important for interpretations of the calculated results.

Figure 5 (a) shows the typical example of charge density distribution of the CP state for  $U = 1t$  and  $V = 0$ , and Fig. 5 (b) displays the  $z$ -component of spin density distribution of the SP state for  $U = 4t$  and  $V = 0$ . The maximum of the charge density is 0.41 in Fig. 5 (a), and that of the spin density is 0.38 in Fig. 5 (b). The polarization of charge is localized along the upper and lower edge sites in Fig. 5 (a). It is extended over the system in Fig. 2 (a). The change of the distribution patterns comes from the different kinds of atoms in the inner region of the nanoribbon. Fig. 5 (b) shows the spin density distributions of the SP state. The alternations of spins are quite strong, as we have found in Fig. 2 (b). The spin polarization is less dependent on the site energy difference, in contrast to the charge polarization distribution. Similarly, spatial enhancement of the CP and SP along the two edges is obtained in Figs. 5 (a) and (b), too. This is the effect due to the presence of the edge states.

Figure 6 shows the phase diagram between the CP and SP states, for the system with  $N = 4$  and  $L = 40$ . The phase boundary means the first order phase transition. The dashed line, the strong correlation limit  $V = (NU + E_N)/(3N - 1) = (4U - 0.8t)/11$ , approaches to the bold

line, when  $U$  and  $V$  become larger. We find the enhanced area of the CP state, as in Fig. 3 of the BN ribbon. The system will exhibit charge polarizations for the realistic values of the interactions, too. The decrease of the slope of the dashed line between Figs. 3 and 6 is due to the decrease of the number of B and N atoms, off course.

Finally, we look at the electric capacitance of the BCN system. The calculations are done for the system size  $L = 20$ , and the results are shown in Fig. 7. We take two parameter sets of Coulomb interactions. The system is in the CP state for these parameters. We obtain the almost inversely proportional behaviors of the capacitance as functions of the ribbon width again. This is due to the strong charge excitation energy gap. Quantitatively, the magnitude is larger than that of Fig. 4, due to the fact that the inner region of the ribbon is composed of carbon, and the local energy gap is smaller than that of the BN system case.

## V. Summary

The charge and spin polarized states have been discussed using the extended Hubbard model for BN and BCN nanotubes and ribbons. Next, the electric capacitance has been calculated in order to test the nano-functionalities of the system. Due to the presence of the strong site energies, the CP state overcomes the SP states, giving the large difference of the phase diagram in comparison with the calculations of graphite system. The electronic structures of the BN and BCN systems are always like of semiconductors. The capacitance calculated for the CP state with the realistic values of the Coulomb interactions is inversely proportional to the distance between the positive and negative electrodes, reflecting the presence of the charge excitation energy gap.

## Acknowledgments

This work has been supported by NEDO under the Nanotechnology Program.

## References

- [1] S. Iijima, *Nature* **354**, 56 (1991).
- [2] R. Saito, G. Dresselhaus, and M. S. Dresselhaus, “Physical Properties of Carbon Nanotubes”, (Imperial College Press, London, 1998).
- [3] M. Fujita, K. Wakabayashi, K. Nakada, and K. Kusakabe, *J. Phys. Soc. Jpn.* **65**, 1920 (1996).
- [4] A. Yamashiro, Y. Shimo, K. Harigaya, and K. Wakabayashi, *Phys. Rev. B* **68**, 193410 (2003).
- [5] A. Rubio, J. L. Corkill, and M. L. Cohen, *Phys. Rev. B* **49**, 5081 (1994).
- [6] X. Blase, A. Rubio, S. G. Louie, and M. L. Cohen, *Europhys. Lett.* **28**, 335 (1994).
- [7] P. Král, E. J. Mele, and D. Tománek, *Phys. Rev. Lett.* **85**, 1512 (2000).
- [8] J. C. Charlier *et al.*, *Nano Lett.* **2**, 1191 (2002).
- [9] M. Terrones *et al.*, *Mater. Today* **7** (10), 30 (2004).
- [10] N. Nakaoka and K. Watanabe, *Eur. Phys. J. D* **24**, 397 (2003).
- [11] K. Wakabayashi and K. Harigaya, *J. Phys. Soc. Jpn.* **72**, 998 (2003).
- [12] T. Yoshioka, H. Suzuura, and T. Ando, *J. Phys. Soc. Jpn.* **72**, 2656 (2003).

## Figure Captions

Fig. 1. Schematic structures of the (a) BN and (b) BCN ribbons with zigzag edges. The filled, shaded, and open circles are B, C, and N sites, respectively. The number of zigzag lines, which are parallel to the  $y$ -axis, is denoted as  $N$ . The total number of atoms along the zigzag line is  $L$ . Periodic boundary condition is imposed to the  $y$ -direction. The number of the B atoms along the upper edge and that of the N atoms along the lower edge are  $L/2$ .

Fig. 2. (a) Charge density distribution of the charge-polarized (CP) state for  $U = 1t$  and  $V = 0$ , and (b) the  $z$ -component of spin density distribution of the spin-polarized (SP) state for  $U = 4t$  and  $V = 0$ , on the zigzag BN ribbon with  $4 \times 20$  sites. The filled and open circles show positive and negative densities. Their radii are proportional to the magnitudes of the charge or spin densities: the maximum is 0.60 in (a) and 0.35 in (b).

Fig. 3. The phase diagram on the  $U$ - $V$  plane of the zigzag BN ribbon with  $4 \times 40$  sites. The bold line is the phase boundary, and the dashed line is the strong correlation limit.

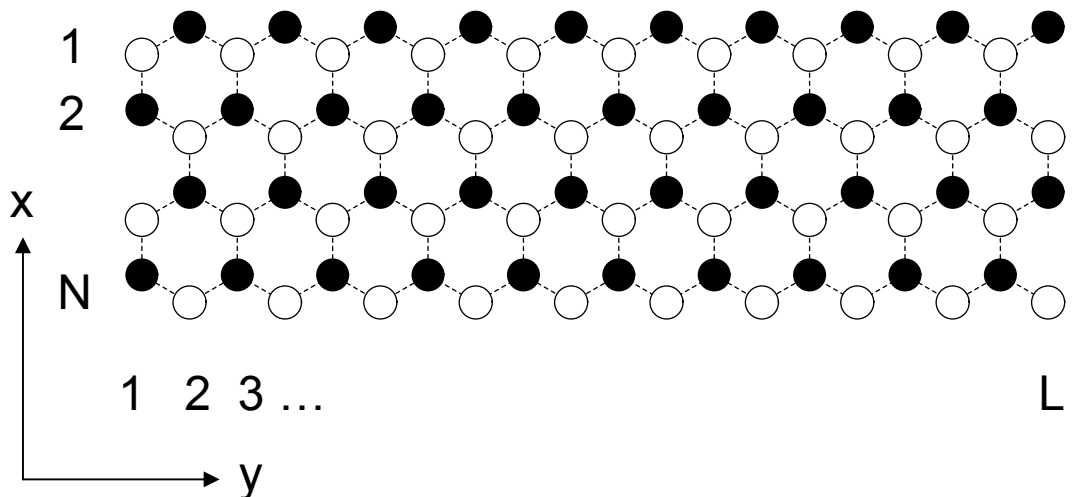
Fig. 4. The electric capacitance calculated for the CP state of the zigzag BN ribbons at  $U = 0$ ,  $1t$ , and  $2t$  with  $V = 0$ . The ribbon length is  $L = 20$ . The magnitudes of (a) the capacitance and (b) its inverse are plotted against the ribbon width in the scale of Å.

Fig. 5. (a) Charge density distribution of the charge-polarized (CP) state for  $U = 1t$  and  $V = 0$ , and (b) the  $z$ -component of spin density distribution of the spin-polarized (SP) state for  $U = 4t$  and  $V = 0$ , on the zigzag BCN ribbon with  $4 \times 20$  sites. The filled and open circles show positive and negative densities. Their radii are proportional to the magnitudes of the charge or spin densities: the maximum is 0.41 in (a) and 0.38 in (b).

Fig. 6. The phase diagram on the  $U$ - $V$  plane of the zigzag BCN ribbon with  $4 \times 40$  sites. The bold line is the phase boundary, and the dashed line is the strong correlation limit.

Fig. 7. The electric capacitance calculated for the CP state of the zigzag BCN ribbons at  $U = 0$  and  $1t$  with  $V = 0$ . The ribbon length is  $L = 20$ . The magnitudes of (a) the capacitance and (b) its inverse are plotted against the ribbon width in the scale of Å.

(a)



(b)

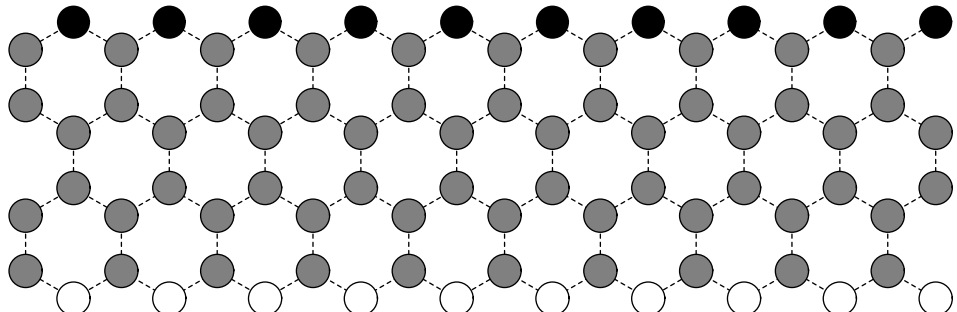
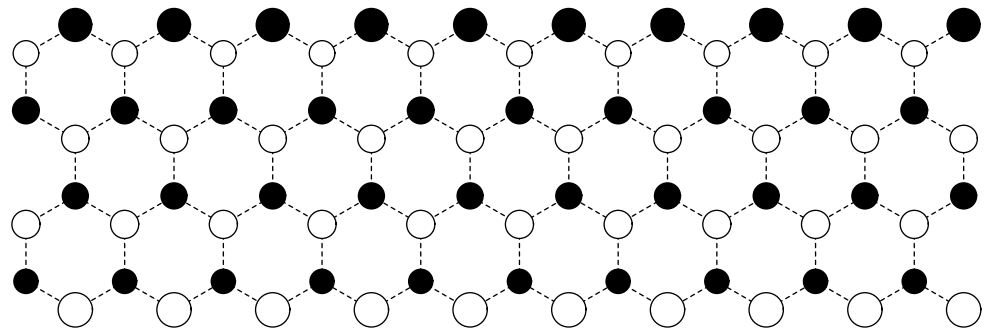


Fig. 1



(a)



(b)

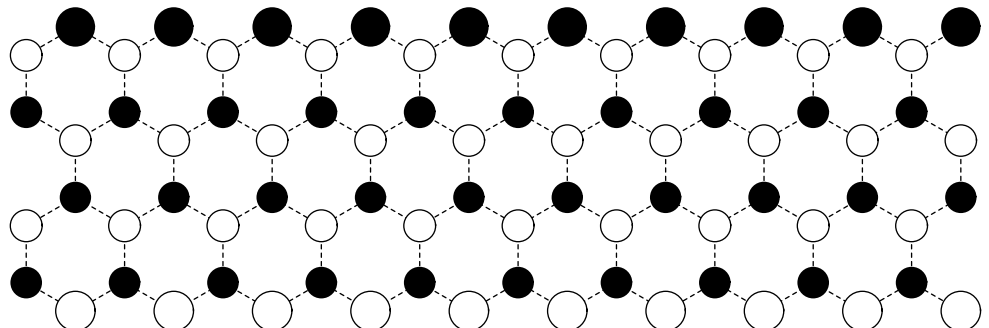
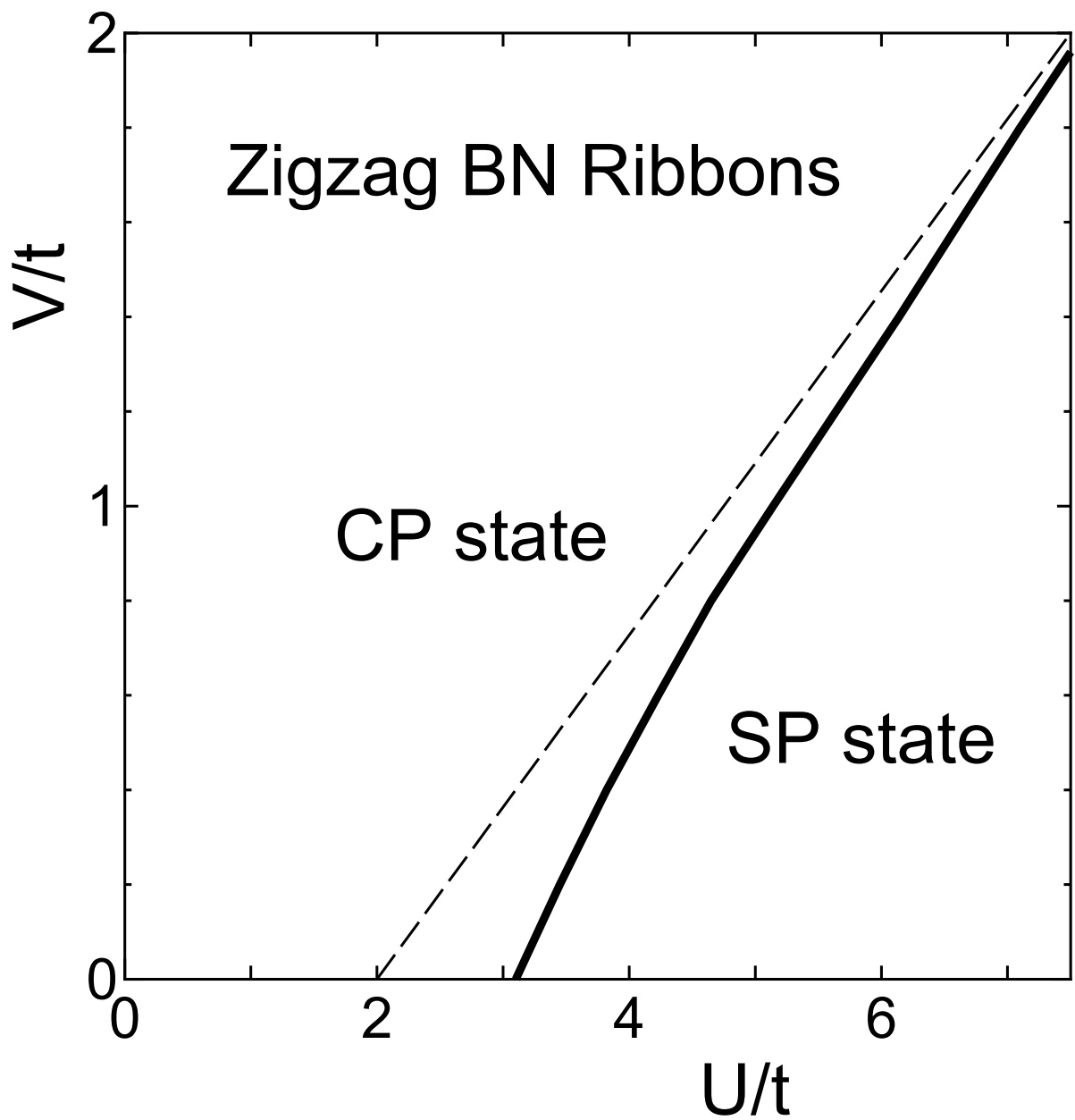
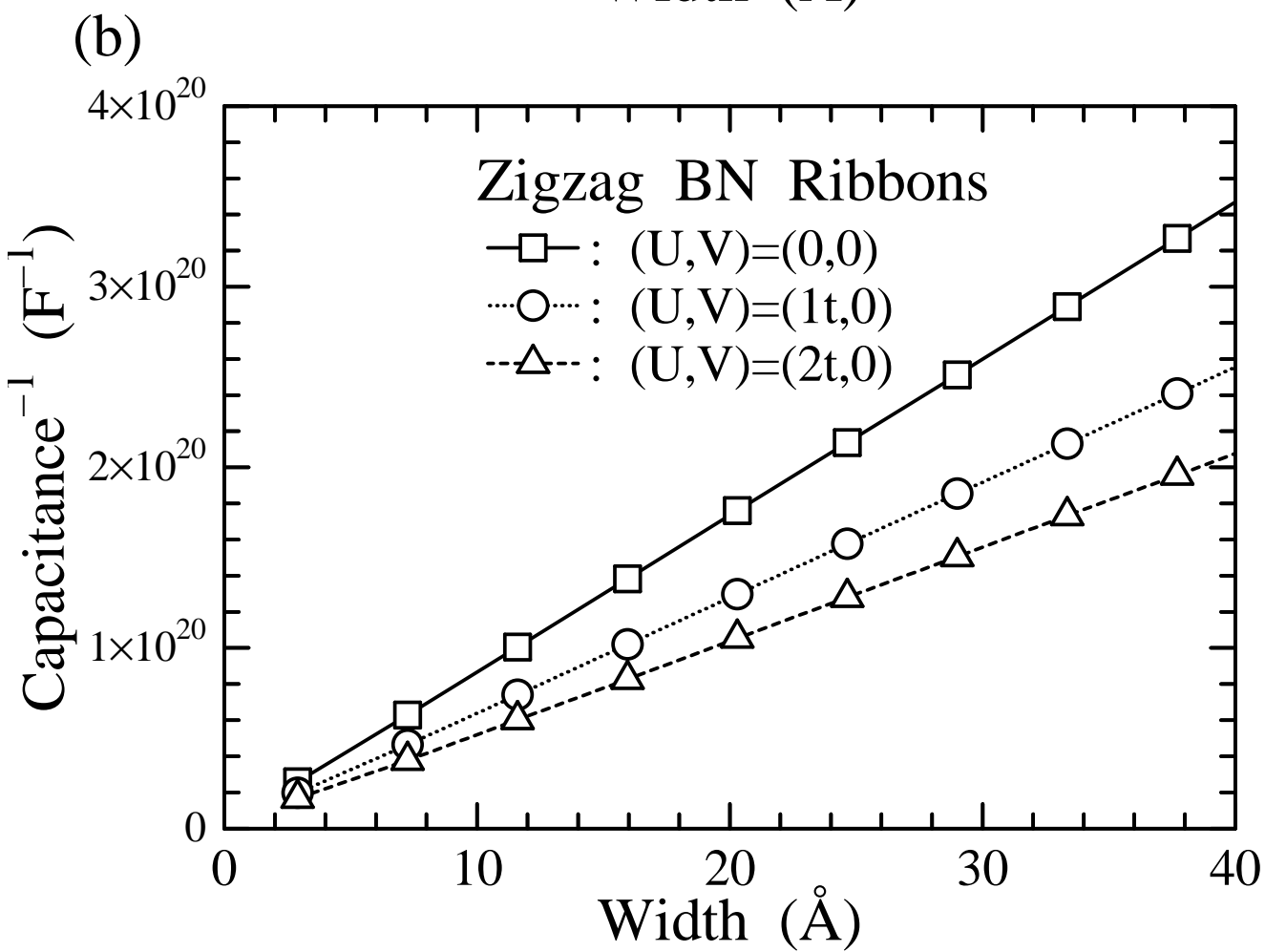
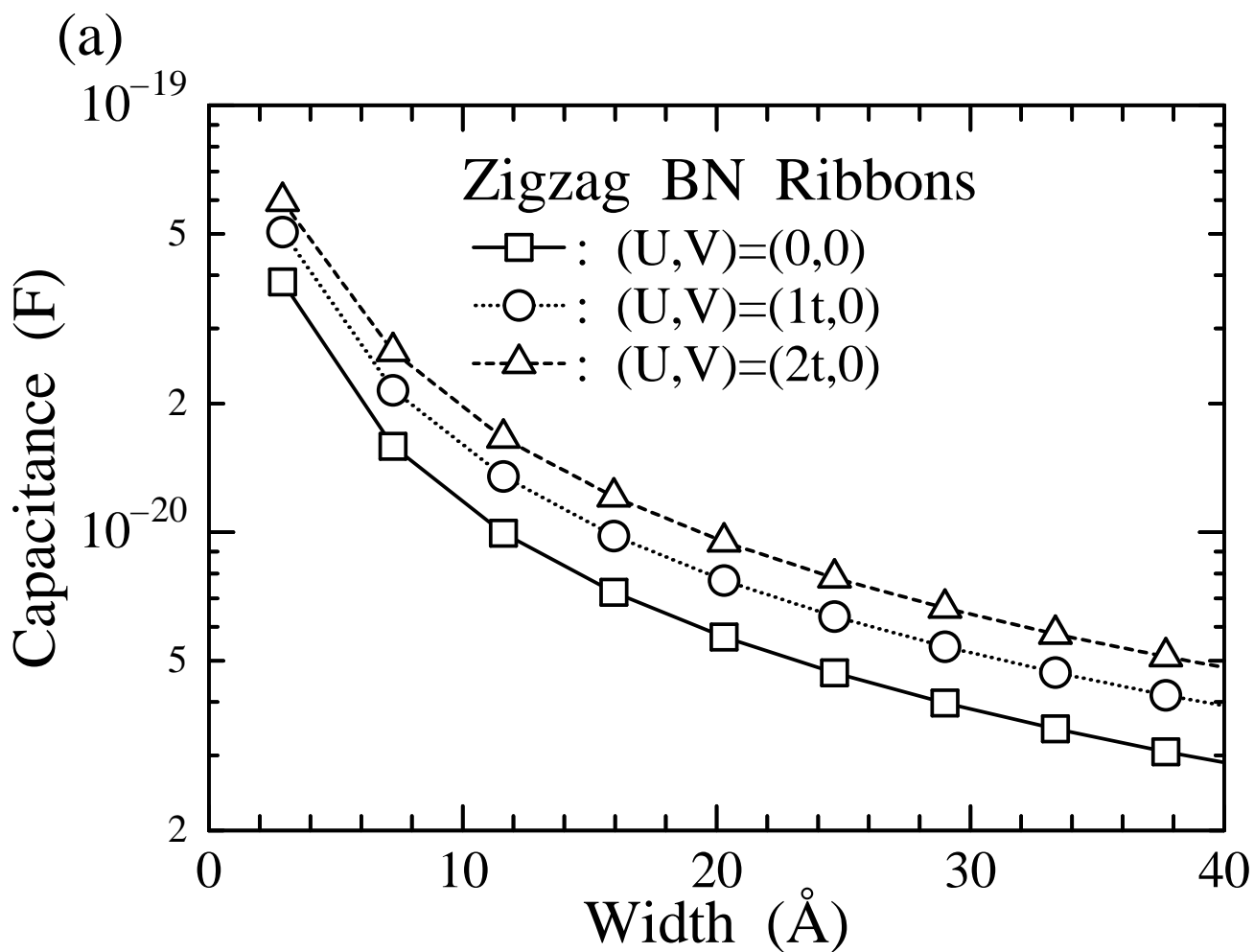


Fig. 2



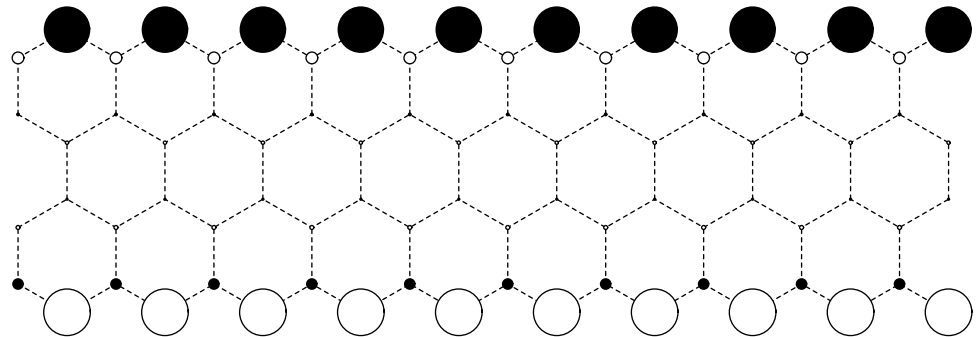








(a)



(b)

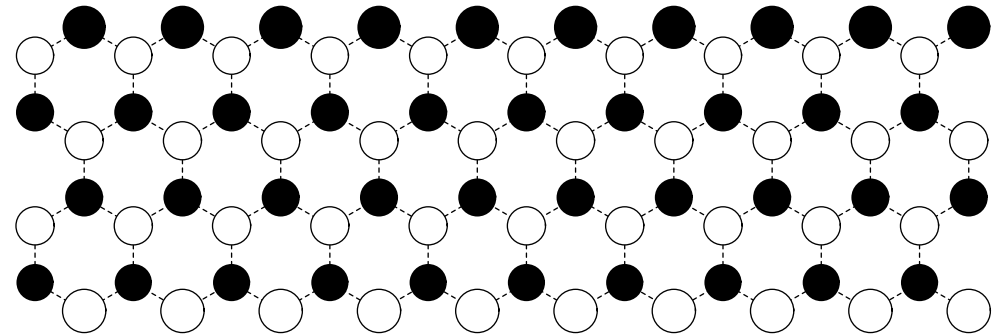


Fig. 5



